Published in final edited form as:
JAMA Ophthalmol. 2013 July ; 131(7): 903–911. doi:10.1001/jamaophthalmol.2013.2065.

Superselective Intraophthalmic Artery Chemotherapy in a Nonhuman Primate Model:

Histopathologic Findings

Brian C. Tse, MD, **Jena J. Steinle, PhD**, **Dianna Johnson, PhD**, **Barrett G. Haik, MD**, and **Matthew W. Wilson, MD**

Department of Ophthalmology, Hamilton Eye Institute (Drs Tse, Steinle, Johnson, Haik, and Wilson), and Department of Anatomy and Neurobiology (Drs Steinle and Johnson), University of Tennessee Health Science Center, Memphis; and Division of Ophthalmology, Departments of Surgery (Drs Haik and Wilson) and Pathology (Dr Wilson), St Jude Children's Research Hospital, Memphis

Abstract

Importance—We describe the histopathologic findings in a nonhuman primate (NHP) model of superselective intraophthalmic artery chemotherapy (SSIOAC), detailing ocular and orbital vascular adverse effects.

Objective—To further document, using comprehensive ocular and orbital histopathology, previously reported toxic effects observed with real-time ophthalmoscopy during SSIOAC in a NHP model.

Design—Comparative interventional case series.

Setting—Preclinical trial approved under the guidelines of the Institutional Animal Care and Utilization committee.

Participants—Six adult male rhesus macaques (*Macacca mulatta*).

Interventions—The right eye of each NHP was treated with 3 cycles of SSIOAC using either melphalan (5 mg/30 mL) or carboplatin (30 mg/30 mL). Both eyes in each animal were enucleated 6 hours after the final procedure, before euthanasia and formalin perfusion of the NHP; we then performed orbital dissection of the arterial vasculature and optic nerves.

Main Outcome Measures—Histopathologic examination of the eyes, optic nerves, and orbital vessels of the 6 treated NHPs.

Correspondence: Matthew W. Wilson, MD, Hamilton Eye Institute, University of Tennessee Health Science Center, 930 Madison Ave, Room 476, Memphis, TN 38103 (mwilson5@uthsc.edu).

Author Contributions: *Study concept and design*: Haik and Wilson. *Acquisition of data*: Tse and Wilson. *Analysis and interpretation of data*: All authors. *Drafting of the manuscript*: Tse, Johnson, and Wilson. *Critical revision of the manuscript for important intellectual content*: All authors. *Obtained funding*: Haik and Wilson. *Administrative, technical, and material support*: All authors. *Study supervision*: Wilson.

Additional Contributions: Alan Stitt, PhD (Queen's University, Belfast, Ireland) provided assistance in transmission electron microscopic analyses of the retinal vasculature.

Conflict of Interest Disclosures: None reported.

Results—We found leukostasis with retinal arteriole occlusion in all treated eyes. Retinal endothelial cells stained positive for 2 inflammatory markers, intercellular adhesion molecule 1 and interleukin 8. Transmission electron microscopy revealed occlusion of the retinal vessels with ultrastructural changes in the endothelial cells and surrounding pericytes. Additional findings included nerve fiber layer infarcts, central retinal artery thrombosis, hypertrophy and occlusion of choroidal arteries with disruption of the internal elastic lamina, patchy choroidal inflammation, and birefringent intravascular foreign bodies. Orbital findings included ophthalmic artery and central retinal artery wall dissection, fracturing of the internal elastic lamina, intimal hyperplasia, and eyelid vessel damage. Optic nerves displayed hemorrhage, leukostasis, and foreign body crystallization. Control eyes, optic nerves, and orbital vessels were normal.

Conclusions and Relevance—Histopathologic examination of our nonhuman primate model for SSIOAC revealed significant toxic effects in the ocular and orbital vasculature. These findings substantiate previous observations with real-time retinal imaging and parallel reported vascular toxic effects in children with retinoblastoma treated with SSIOAC.

Superselective intraophthalmic artery chemotherapy (SSIOAC) has come to the forefront in the treatment of retinoblastoma, without the benefit of preclinical modeling.[1] Real-time ophthalmoscopic observations of SSIOAC in a nonhuman primate (NHP) model were described elsewhere.[2] Multiple acute ocular vascular sequelae were documented, including ophthalmic artery (OA) thrombosis, narrowing of the OA and retinal arteries, pulsatile optic nerve and retinal edema, retinal artery sheathing and precipitates, and choroid blanching and hypoperfusion.

Few reports have detailed the histopathologic changes associated with SSIOAC.[3-5] Recently, Eagle and colleagues[6] reported the histopathologic findings of 8 enucleated eyes after treatment of retinoblastoma with SSIOAC. Indications for enucleation included poor tumor response to therapy, recurrent vitreous seeding, anaphylaxis, neovascular glaucoma, and persistent retinal detachment. The study revealed evidence of retinal and choroidal atrophy induced by vascular compromise, intravascular birefringent foreign body material, and vessel thrombosis. Three of the eyes, however, had received plaque brachytherapy, external beam radiotherapy, or cryotherapy in addition to SSIOAC.

The principal aims of our NHP study were to (1) document the ocular findings during infusion with real-time ophthalmic imaging; (2) measure the vitreous and systemic chemotherapy pharmacokinetics; (3) describe the histopathologic findings in treated eyes; and (4) validate our model by comparing orbital vascular anatomy in the NHP model with that in a 2-year-old child. The findings for aim 1 have already been published,[2] and those for aims 2 and 4 will be reported separately. To our knowledge, our present study, focusing on aim 3, is the first to examine histopathologic findings in the eyes, optic nerves, and orbital vasculature after SSIOAC in an NHP model.

METHODS

A detailed description of the SSIOAC technique used in this study was provided elsewhere.[2] In brief, we randomly assigned 6 adult male Rhesus macaques (*Macacca mulatta)* to 1 of 2 treatment cohorts (right eye received treatment and the contralateral eye served as the

control), receiving either melphalan (5 mg/30 mL) or carboplatin (30 mg/30 mL). Six hours after the final chemotherapy infusion (3 cycles at 3-week intervals), we enucleated the globes, injected them with 1 mL of 0.04% paraformaldehyde, and then placed them in 10% neutral buffered formalin for at least 48 hours before gross examination. Immediately after enucleation, we euthanized the animals and perfused them with 10% neutral buffered formalin to fixate the orbital tissues. Approval for the study and institutional guidelines were obtained and followed as required by the Institutional Animal Care and Use Committee at the University of Tennessee Health Science Center, Memphis.

OCULAR PATHOLOGY SECTION PREPARATION

During gross examination, we opened the globes vertically and removed the temporal and nasal caps. We processed and sectioned (temporal to nasal, at least 500 sections per eye) the pupil–optic nerve section for routine light microscopy, stained every fifth slide with hematoxylin-eosin, and chose appropriate unstained sections for further histochemical (elastin stain) and immunohistochemical study.

IMMUNOHISTOCHEMISTRY

We used rabbit monoclonal antibodies reactive to the Cterminus of the human intercellular adhesion molecule 1 protein (ICAM-1; concentration optimized at 1:200) (TA307840; OriGene Technologies) and reactive to the residues surrounding valine 68 of the human interleukin 8 protein (IL-8; concentration optimized at 1:1000) (NBP1-19757; Novus Biologicals). Heat-induced epitope retrieval was used on the paraffin sections. A rabbit-on-rodent polymer–horseradish peroxidase (RMR622L; BioCare Medical) was used for antibody detection with the chromogen diaminobenzidine (TA-125-HDX; Thermo Shandon) and hematoxylin counterstain.

TRANSMISSION ELECTRON MICROSCOPY

On gross examination, we placed the nasal and temporal caps of each eye in 4% paraformaldehyde fixative overnight at 4°C. After dissection, we placed the samples into a solution of 2.5% glutaraldehyde and 2% paraformaldehyde in 0.1 mol/L sodium cacodylate at 4°C. We postfixed the samples with osmium tetroxide, followed by staining with 2% uranyl acetate, dehydratation, embedding in epon, and polymerization. Finally, we prepared 80-nm-thick sections and collected them onto copper grids for transmission electron microscopic analysis.

ORBITAL PATHOLOGY SECTION PREPARATION

Using a 15-blade scalpel, we reflected the scalp of the NHP to expose the skull and then removed the calvarium with a bone saw. We removed the brain, carefully preserving the circle of Willis and optic nerves. We resected dura from the skull base and used rongeurs to remove the bone roofs of the orbit and optic canal. Using Westcott scissors, we severed the levator and superior rectus muscles from the insertions, reflected the muscles, and exposed the intraconal contents. Dissecting orbital fat off the orbital vasculature with jeweler’s forceps allowed us to identify the OA and its branches without traumatizing the vessels. Then we carefully removed optic nerves from the optic canal to reveal the origin of the OA.

Finally, we placed the optic nerves and orbital arterial tree (removed beginning at the origin of the OA en bloc from the right and left orbits of each animal) in 10% neutral buffered formalin.

We identified, inked, and isolated the ophthalmic, central retinal, frontal and lacrimal arteries, then sectioned, embedded on edge, and serially sectioned each artery and optic nerve. One animal, MEL 561, had had persistent swelling and erythema of the right upper eyelid since the initial SSIOAC, so we removed the right upper eyelid intact, placed it into 10% neutral buffered formalin, and then trisected and prepared it for pathologic examination, as already described.

RESULTS

OCULAR PATHOLOGY

The eyes in our NHP model measured 19 × 19 × 19 mm with no gross abnormalities. No pathologic abnormalities were observed in the control eyes. In Table 1, we delineate all ocular pathologic findings (see also Figures 1, 2, 3, 4, 5, and 6). In the treated eyes, we found localized endothelial immunohistochemical staining for ICAM-1 and staining for IL-8 in the retinal endothelial cells and surrounding neurosensory retina (Figure 2). We found less robust staining in the control eyes. Birefringent foreign bodies found in the choroidal and short posterior ciliary arteries of 3 treated eyes were approximately 20 μm in diameter and appeared to be aggregates of smaller particles (Figure 5). In 1 central retinal artery (CRA), a thrombus was organized with fibrovascular tissue retracted from the vessel wall as the vessel recanalized. The corresponding retina showed loss of the ganglion cell layer and was thinner than the control eye (Figure 6).

Vascular ultrastructural changes of SSIOAC-treated and untreated eyes were assessed with electron microscopy. Retinal vessels of nontreated eyes showed clear lumina devoid of blood cells or cellular debris, whereas many vessels of treated eyes were occluded by red blood cell aggregates, macrophages, and membranous debris. Small endothelial cell projections were commonly observed, and pericytes displayed swelling and disorganization of intracellular organelles (Figure 7).

ORBITAL PATHOLOGY

We examined all orbital vasculature except that of 1 control side; the initial left-sided dissection in 1 animal (MEL 330) was not suitable for histologic examination. We examined the optic nerves in 5 of the 6 NHPs; the optic nerves in 1 animal (MEL 561) were not suitable for histologic examination. Examination findings in the control orbital vasculature and optic nerves were normal in all NHPs. Our orbital pathologic findings are presented in Table 2 and Figures 8, 9, and 10. One animal was noted to have a dissection within the wall of the distal OA that propagated anterior into the CRA, with red blood cells noted within the dissection space (Figure 8) and CRA wall thickening in comparison to the control side. A birefringent foreign body was found on examination of the optic nerves, similar in appearance to those previously described (Figure 5). In the right upper eyelid of MEL 561, which developed swelling after the first drug infusion and persisted through the termination

of the study, we found evidence of medium-vessel thrombosis and inflammatory cells within the tarsal conjunctiva (Figure 10).

DISCUSSION

In the treatment of retinoblastoma, SSIOAC delivers localized, concentrated chemotherapy to the OA in the hopes of minimizing systemic adverse effects. Reports to date are predominantly single-center retrospective studies on variations in technique.[1,7,8] Modifications in OA cannulation, the chemotherapeutic agent, and infused concentration may be an attempt to mitigate reported complications as SSIAOC has become more commonplace. Sectoral choroidal occlusion, retinal arteriolar emboli, retinal detachment, vitreous hemorrhage, transient retinal ischemia, and OA obstruction are the ocular adverse effects, whereas periocular inflammation and edema, cranial nerve III palsies, and eyelash loss are the orbital and adnexal adverse effects.[9-14] In absence of preclinical modeling, these potential toxic effects were not anticipated. Herein, we document ocular and orbital vascular histopathologic findings in 6 NHPs treated with SSIOAC.

Previous studies have detailed the histopathologic findings in eyes with retinoblastoma treated with SSIOAC. These studies principally focused on residual viable tumor[4,5]; however, Eagle and coworkers[6] documented findings attributed to toxic effects of SSIOAC in 8 eyes. These included ischemic atrophy involving the outer retina and choroid (n = 4), orbital vascular occlusion and subendothelial smooth muscle hyperplasia (n = 1), and thrombosed blood vessels involving the retrobulbar ciliary arteries (n = 5), scleral emissary canals (n = 1), small choroidal vessels (n = 1), and CRA (n = 1). Intravascular birefringent foreign material was noted in 5 eyes and classified as cellulose fibers (n = 3), synthetic fabric fibers (n = 1), or unknown composition (n = 2).

We found similar pathologic findings in our 6 NHP eyes treated with SSIOAC. Retinal arteriole occlusion, endothelial cell damage, and leukocyte adhesion were prominent findings in each of the eyes. Thrombi, 1 of which had organized, were noted in the CRA of 4 eyes. Immunohistochemical expression of ICAM-1 and IL-8 by retinal endothelial cells—as well as endothelial cell sloughing, pericyte disorganization, and membranous debris within the vascular spaces of the treated eyes—support our hypothesis, derived from prior in vitro studies, of a drug-induced retinal endothelial cell inflammatory response with secondary leukostasis leading to vascular occlusion. [15] We also noted intravascular birefringent foreign bodies approximately 20 μm in diameter within the retinal, choroidal, and short posterior ciliary arteries of 3 animals and within the optic nerve of another. However, we believe these particles are drug precipitates within smaller-caliber vessels—aggregates of the 5-μm particles described elsewhere in hyperconcentrated infusate. [2]

Although animal models of intra-arterial therapy exist— specifically models involving regional and hepatic perfusion—and have been used to document local toxic effects, clinical studies in patients have shown that vasculopathic toxic effects may occur in response to highdose systemic and regional melphalan perfusion.[16,17] Extrapolating from these studies, one could predict regional vascular toxicity. However, the nature and extent of such toxic effects have not been described before our study. We are unaware of animal or clinical

studies in which this concentration of melphalan has been infused in this manner in an artery of this size for this duration. We believe that melphalan, and the aggregates that form in vivo, account for the pathologic effects in smaller vessels, principally thrombosis, leukostasis, and occlusion. As already discussed, in vitro findings in retinal endothelial cells support drug-mediated toxicity.[15] Finally, since completion of the present study, other investigators have reported similar findings in children treated with SSIOAC.[18]

Although prior studies have examined ocular histopathologic findings after SSIOAC, we are unaware of any study with detailed orbital histopathologic findings. We documented 3 significant changes in the orbital vasculature: intimal hyperplasia, fracturing of the internal elastic lamina, and arterial wall dissection. Each represents a unique response to mechanical trauma from SSIOAC, specifically the turbulent flow created by manual pulsatile infusion. Intimal hyperplasia is a well-known physiologic response associated with vascular injury,[19,20] and fracturing of the internal elastic lamina is another indicator of vascular damage.[19] Our most important finding was an arterial dissection involving the distal OA and CRA. To our knowledge, ophthalmic and CRA dissection after SSIOAC has not been previously reported in the literature. An arterial dissection, by definition, is a traumatic event. As for the etiology in our NHP model, we believe that flow turbulence and vasculature stretch within the OA during pulsatile infusion caused an intimal tear. We believe it is less likely that mechanical trauma from cannulation of the OA led to the dissection, because the dissection began in the distal portion of the OA and propagated anterior to the CRA. In our procedures, the microcatheter was advanced no more than 2 mm past the ostium of the OA.[2]

Our study is also the first to provide histopathologic findings for the transient eyelid erythema and edema commonly observed after SSIOAC,[3,11,12,21] with 13 of 17 patients affected in 1 study.[11]Wefound evidence of a thrombus within an upper eyelid vessel in the animal that had persistent swelling and redness after the initial procedure. The presence of the thrombus, leukostasis, and birefringent crystals elsewhere in the orbital arterial tree suggest drug-related toxic effects similar to those observed in the retinal, choroidal, and short posterior ciliary arteries.

In contrast to prior histopathologic findings in eyes treated with SSIOAC, our treated NHP eyes had no coexisting pathologic conditions or prior treatments. All contralateral eyes and orbital vessels were normal. We believe our histopathologic findings are the direct sequelae of SSIOAC, reflecting mechanical trauma from infusion and toxic effects from chemotherapy. Our findings are expected based on the acute vasculopathies observed with real-time fundus imaging in the same NHP model during SSIOAC.[2] Because we have validated our NHP model, finding comparable diameters of eyes and OAs in a control pediatric population younger than 6 years,[22] our results are directly translatable to children with retinoblastoma. To that end, separate studies by Eagle et al[6] and Shields et al[12] of the histopathologic and clinical findings in eyes of children with retinoblastoma treated with SSIOAC parallel our findings in an NHP model.

In conclusion, histopathologic examination of NHP eyes and orbits treated with SSIOAC revealed widespread vascular damage. Although our findings represent acute toxic effects,

we are concerned about the long-term effects of SSIOAC on ocular and orbital vasculature. Do the observed toxic effects place these eyes at an increased risk of future ischemic or thrombotic events? Prospective, long-term follow-up is needed well after intraocular disease is controlled. Finally, our research stresses the need for further preclinical modeling to address the variables of flow and drug concentration in an attempt to mitigate these ocular and orbital vascular toxic effects.

Acknowledgments

Funding/Support: This study was supported in part by an unrestricted grant to the Department of Ophthalmology, University of Tennessee Health Science Center, Memphis, from Research to Prevent Blindness, Inc, and the St Giles Foundation.

References

1. Abramson DH, Dunkel IJ, Brodie SE, Kim JW, Gobin YP. A phase I/II study of direct intraarterial (ophthalmic artery) chemotherapy with melphalan for intraocular retinoblastoma initial results. Ophthalmology. 2008; 115(8):1398–1404. 1404.e1. published online March 14, 2008. 10.1016/j.ophtha.2007.12.014 [PubMed: 18342944]
2. Wilson MW, Jackson JS, Phillips BX, et al. Real-time ophthalmoscopic findings of superselective intraophthalmic artery chemotherapy in a nonhuman primate model. Arch Ophthalmol. 2011; 129(11):1458–1465. [PubMed: 22084215]
3. Vajzovic LM, Murray TG, Aziz-Sultan MA, et al. Clinicopathologic review of enucleated eyes after intra-arterial chemotherapy with melphalan for advanced retinoblastoma. Arch Ophthalmol. 2010; 128(12):1619–1623. [PubMed: 21149791]
4. Graeber CP, Gobin YP, Marr BP, et al. Histopathologic findings of eyes enucleated after treatment with chemosurgery for retinoblastoma. Open Ophthalmol J. 2011; 5:1–5. [PubMed: 21399766]
5. Kim J, Do H, Egbert P. Enucleated eyes after failed intra-arterial infusion of chemotherapy for unilateral retinoblastoma: histopathologic evaluation of vitreous seeding. Clin Ophthalmol. 2011; 5:1655–1658. [PubMed: 22174572]
6. Eagle RC Jr, Shields CL, Bianciotto C, Jabbour P, Shields JA. Histopathologic observations after intra-arterial chemotherapy for retinoblastoma. Arch Ophthalmol. 2011; 129(11):1416–1421. [PubMed: 21746972]
7. Shields CL, Bianciotto CG, Jabbour P, et al. Intra-arterial chemotherapy for retinoblastoma: report No. 1, control of retinal tumors, subretinal seeds, and vitreous seeds. Arch Ophthalmol. 2011; 129(11):1399–1406. [PubMed: 21670328]
8. Venturi C, Bracco S, Cerase A, et al. Superselective ophthalmic artery infusion of melphalan for intraocular retinoblastoma: preliminary results from 140 treatments. Acta Ophthalmol. 2012 published online January 23, 2012. 10.1111/j.1755-3768.2011.02296.x
9. Munier FL, Beck-Popovic M, Balmer A, Gaillard MC, Bovey E, Binaghi S. Occurrence of sectoral choroidal occlusive vasculopathy and retinal arteriolar embolization after superselective ophthalmic artery chemotherapy for advanced intraocular retinoblastoma. Retina. 2011; 31(3):566–573. [PubMed: 21273941]
10. Shields CL, Shields JA. Retinoblastoma management: advances in enucleation, intravenous chemoreduction, and intra-arterial chemotherapy. Curr Opin Ophthalmol. 2010; 21(3):203–212. [PubMed: 20224400]
11. Vajzovic LM, Murray TG, Aziz-Sultan MA, et al. Supraselective intra-arterial chemotherapy: evaluation of treatment-related complications in advanced retinoblastoma. Clin Ophthalmol. 2011; 5:171–176. [PubMed: 21383945]
12. Shields CL, Bianciotto CG, Jabbour P, et al. Intra-arterial chemotherapy for retinoblastoma: report No. 2, treatment complications. Arch Ophthalmol. 2011; 129(11):1407–1415. [PubMed: 21670326]

13. Gobin YP, Dunkel IJ, Marr BP, Brodie SE, Abramson DH. Intra-arterial chemotherapy for the management of retinoblastoma: four-year experience. Arch Ophthalmol. 2011; 129(6):732–737. [PubMed: 21320950]

14. Muen WJ, Kingston JE, Robertson F, Brew S, Sagoo MS, Reddy MA. Efficacy and complications of super-selective intra-ophthalmic artery melphalan for the treatment of refractory retinoblastoma. Ophthalmology. 2012; 119(3):611–616. [PubMed: 22197434]

15. Steinle JJ, Zhang Q, Thompson KE, et al. Intra-ophthalmic artery chemotherapy triggers vascular toxicity through endothelial cell inflammation and leukostasis. Invest Ophthalmol Vis Sci. 2012; 53(4):2439–2445. [PubMed: 22427570]

16. Samuels BL, Bitran JD. High-dose intravenous melphalan: a review. J Clin Oncol. 1995; 13(7): 1786–1799. [PubMed: 7602368]

17. Lens MB, Dawes M. Isolated limb perfusion with melphalan in the treatment of malignant melanoma of the extremities: a systematic review of randomised controlled trials. Lancet Oncol. 2003; 4(6):359–364. [PubMed: 12788409]

18. Fallaha N, Dubois J, Carret AS, Callejo SA, Hamel P, Superstein R. Real-time ophthalmoscopic findings of intraophthalmic artery chemotherapy in retinoblastoma. Arch Ophthalmol. 2012; 130(8):1075–1077. [PubMed: 22893086]

19. Nobuyoshi M, Kimura T, Ohishi H, et al. Restenosis after percutaneous transluminal coronary angioplasty: pathologic observations in 20 patients. J Am Coll Cardiol. 1991; 17(2):433–439. [PubMed: 1991900]

20. Schwartz RS, Murphy JG, Edwards WD, Camrud AR, Vliestra RE, Holmes DR. Restenosis after balloon angioplasty: a practical proliferative model in porcine coronary arteries. Circulation. 1990; 82(6):2190–2200. [PubMed: 2146991]

21. Abramson DH, Dunkel IJ, Brodie SE, Marr B, Gobin YP. Superselective ophthalmic artery chemotherapy as primary treatment for retinoblastoma (chemosurgery). Ophthalmology. 2010; 117(8):1623–1629. [PubMed: 20381868]

22. Ditta LC, Choudhri AF, Tse BC, et al. Validating a nonhuman primate model of super-selective intraophthalmic artery chemotherapy: comparing ophthalmic artery diameters. Invest Ophthalmol Vis Sci. 2012; 53(12):7791–7794. [PubMed: 23111611]

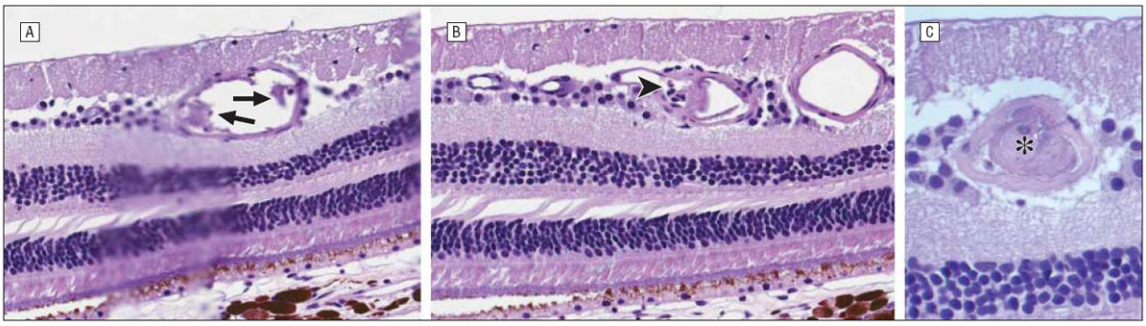

Figure 1.

Hematoxylin-eosin–stained serial sections of retinal arteriole progressing temporally reveal endothelial cell damage (arrows) (original magnification ×80) (A), leukostasis (arrowhead) (original magnification ×80) (B), and occlusion (asterisk) (original magnification ×120) (C) in eye treated with melphalan (MEL 330).

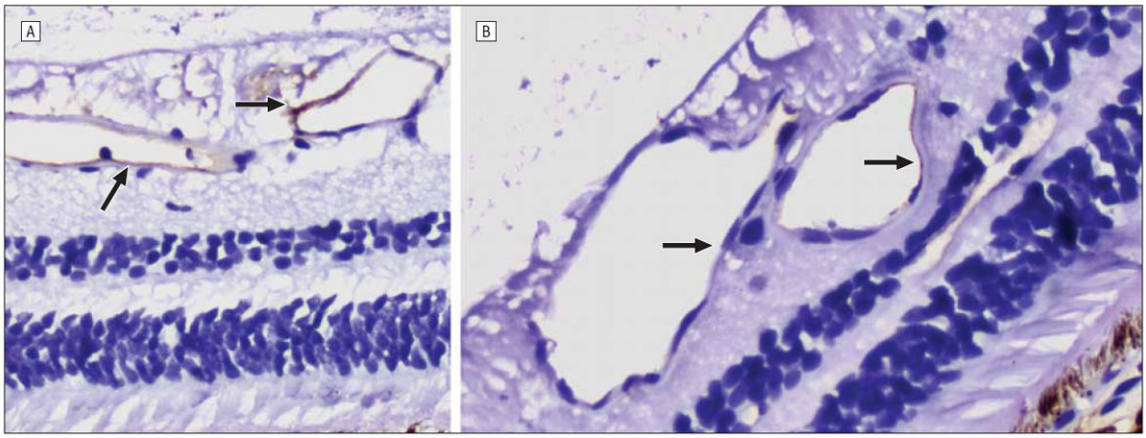

Figure 2.

Intercellular adhesion molecule 1 staining (arrows) was more robust in the carboplatin-treated (A) than in the untreated (B) eye (original magnification ×80; CBP 039). The faint staining seen in the control eye (B) was attributed to systemic distribution of the infused chemotherapeutic agent.

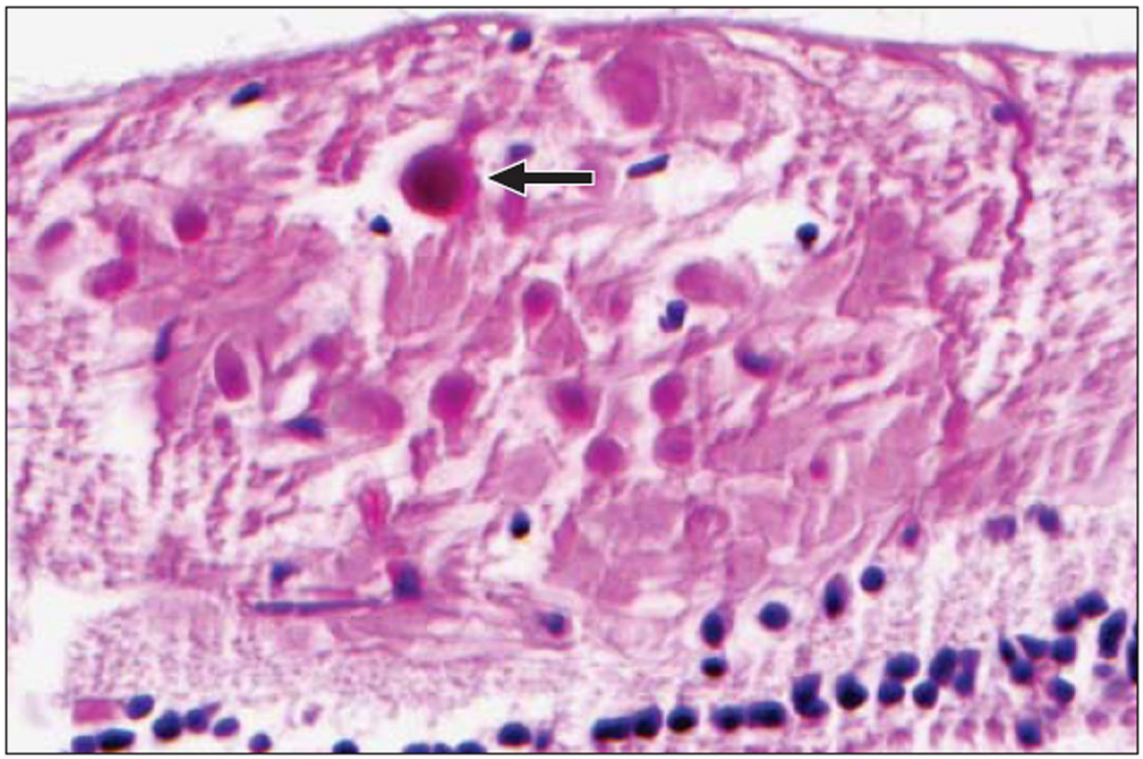

Figure 3.
Nerve fiber layer infarction with cytoid bodies (arrow) in a carboplatintreated eye (hematoxylin-eosin, original magnification ×120; CBP 404).

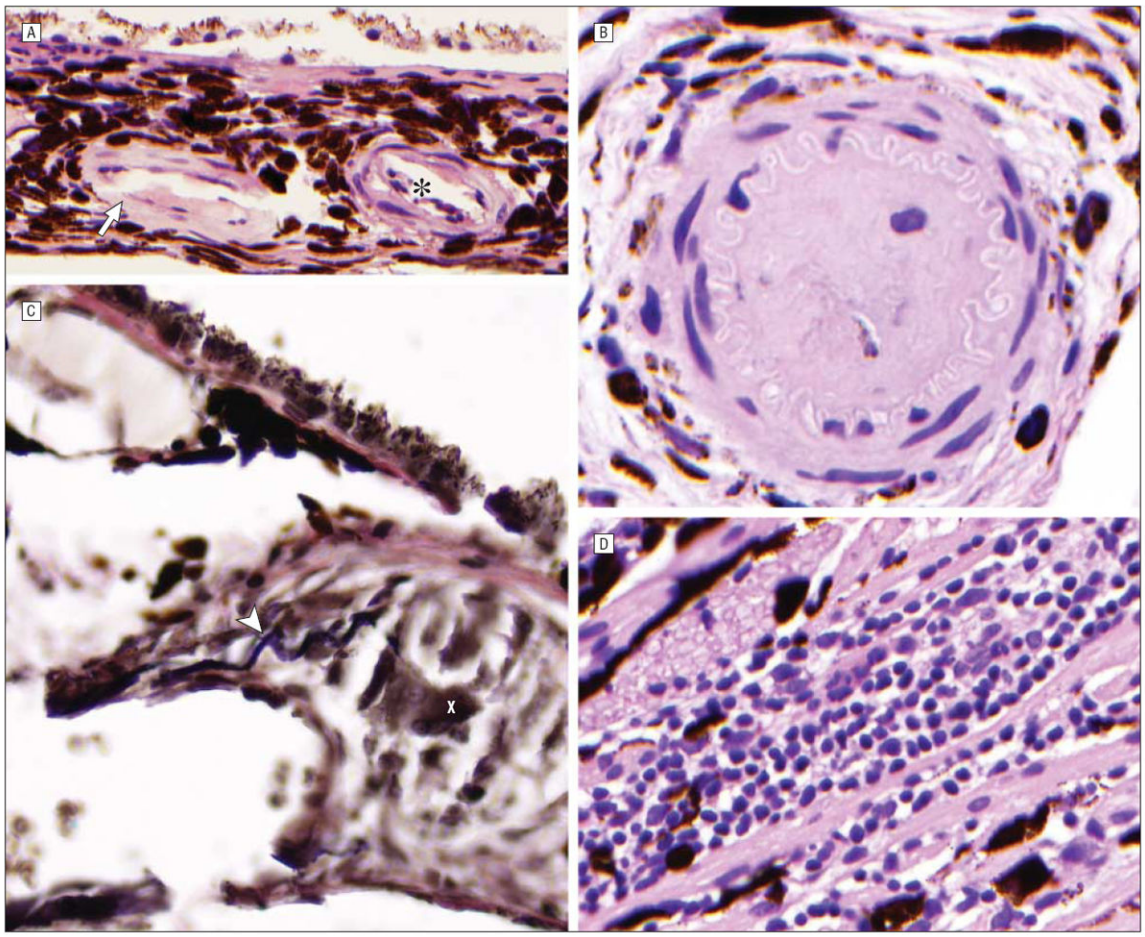

Figure 4.

Findings after melphalan (MEL) treatment included thickening of the choroidal arteriole walls (arrow) with associated leukostasis (asterisk) (hematoxylin-eosin, original magnification ×80; MEL 006) (A) and occlusion of a choroidal arteriole (hematoxylin-eosin, original magnification ×80; MEL 330) (B). In 1 animal treated with carboplatin (CBP 039) elastin stain highlighted disruption of the internal elastic lamina (arrowhead) of a choroidal arteriole, with associated granulomatous inflammation (*X*) (C) (elastin, original magnification ×120) (C) and mixed inflammatory infiltrate in the choroid (hematoxylin-eosin, original magnification ×80) (D).

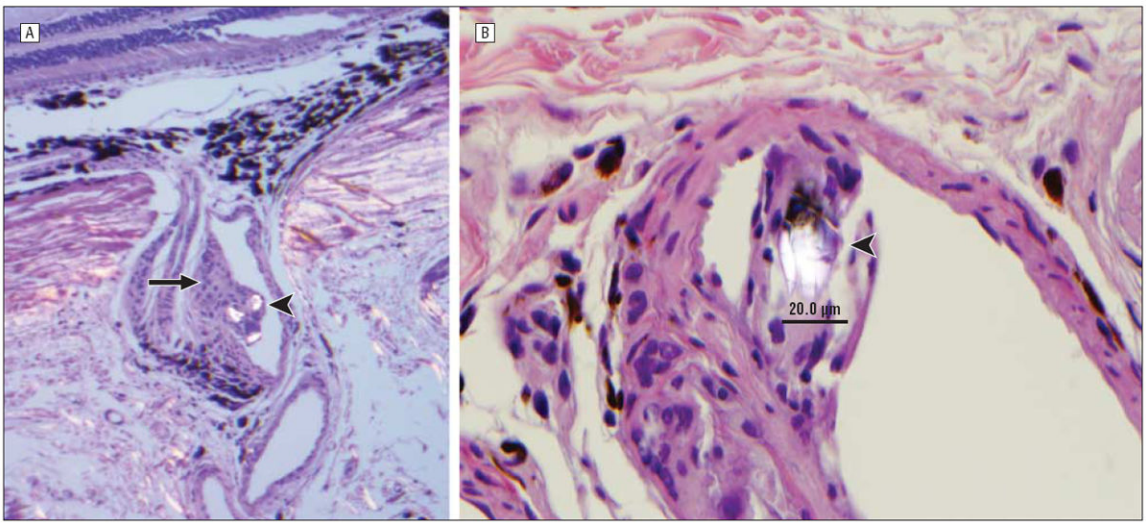

Figure 5.

Findings after melphalan treatment in 1 animal (MEL 330) included partial occlusion (arrow) of a short posterior ciliary artery coursing through the sclera (hematoxylin-eosin, original magnification ×40) (please note birefrigent particles [arrowhead] in lumen vessel) (A) and birefringent foreign bodies (arrowhead) measuring approximately 20 µm (hematoxylin-eosin, original magnification ×80) (B).

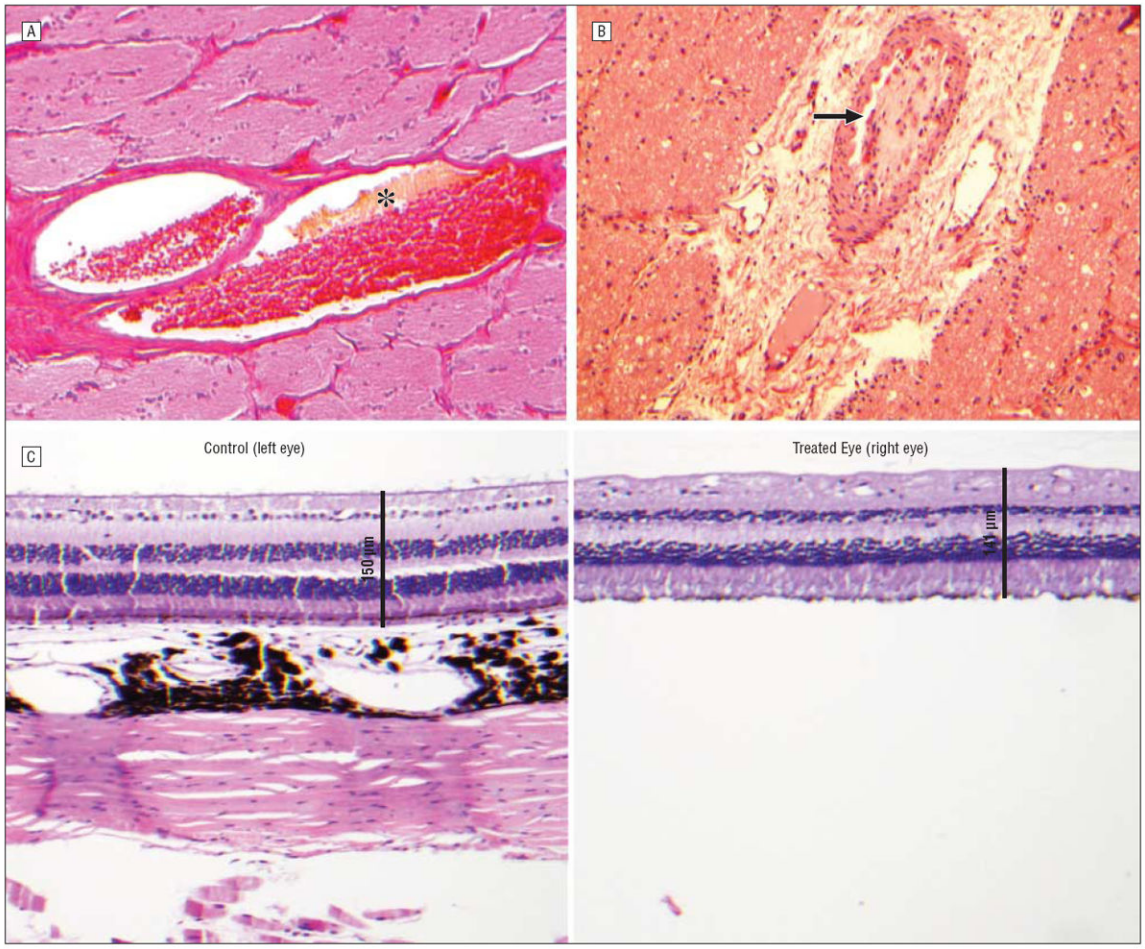

Figure 6.

Findings after carboplatin (CBP) treatments included degradation of erythrocytes (asterisk) with partial thrombus formation in the central retinal artery (hematoxylin-eosin, original magnification ×40; CBP 039) (A); retracted, organized thrombus (arrow) in the central retinal artery (hematoxylin-eosin, original magnification ×40; CBP 328) (B); and, with corresponding loss of the ganglion cell (hematoxylin-eosin, original magnification ×20; CBP 328) (C).

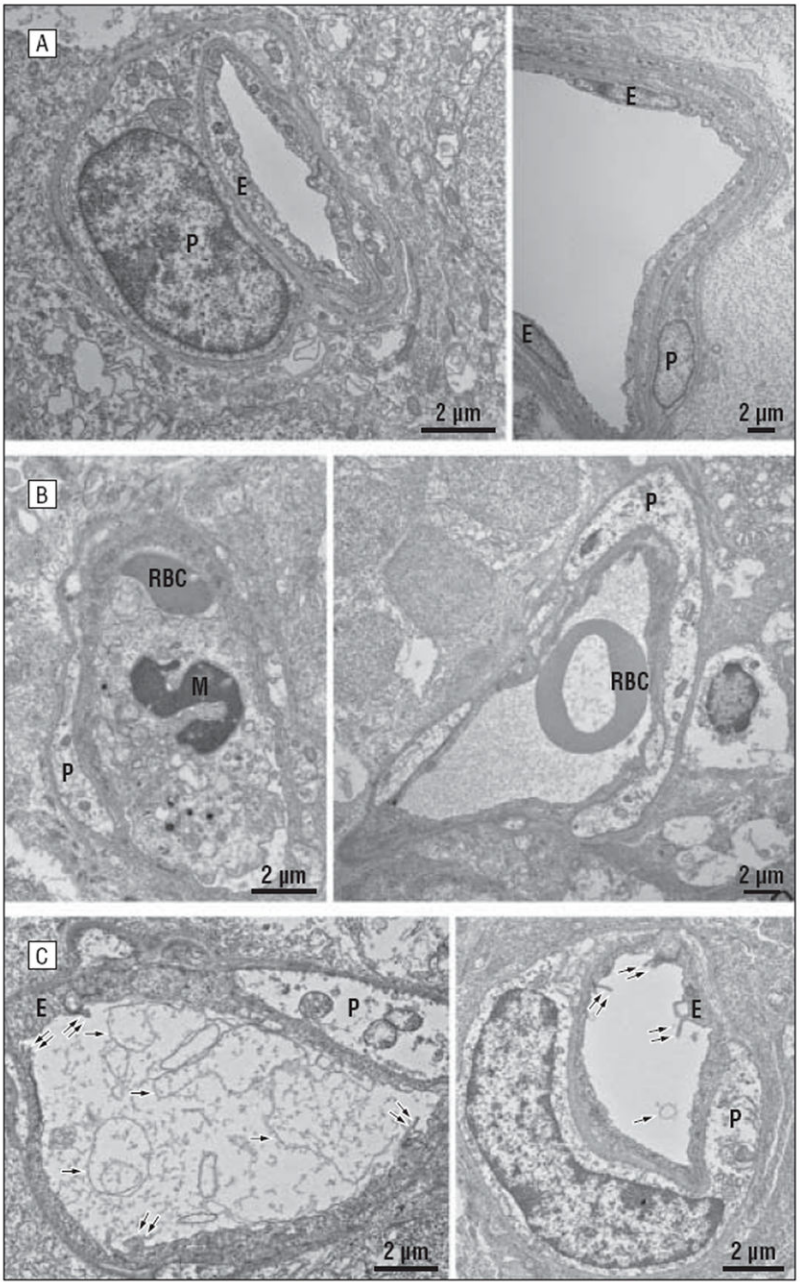

Figure 7.

Transmission electron microscopy. A, Retinal vascular morphology in control eyes. In both small (A1) and large (A2) vessels, the integrity of pericytes (*P*) and vascular endothelial cells (*E*) is well preserved. Vessels show a clear lumen with no blood cells, membrane debris, or endothelial projections. B, Retinal vascular damage in nonhuman primates treated with superselective intraophthalmic artery chemotherapy. B1 and B2, Vessels were often occluded by red blood cells (*RBC*) and macrophagelike cells (*M*). Pericytes (P) were routinely swollen and contained disrupted intracellular organelles. C1 and C2, In lumina that

were clear of cells, membrane debris (single arrows) and extended endothelial projections (double arrows) were commonly observed.

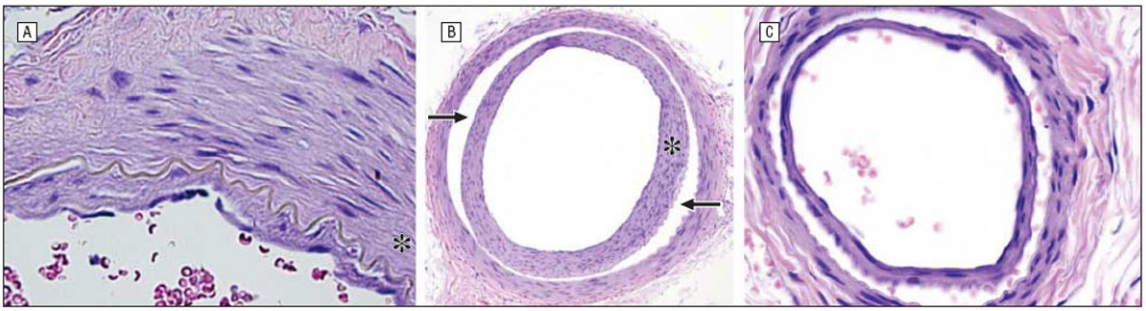

Figure 8.

Traumatic damage after treatment includes intimal hyperplasia (asterisk) of the ophthalmic artery (hematoxylin-eosin, original magnification ×80; MEL 561) (A) and dissection (arrows) of the ophthalmic artery with intimal hyperplasia (hematoxylin-eosin, original magnification ×20; CBP 328) (B) that propagates anteriorly to involve the central retinal artery (hematoxylin-eosin, original magnification ×20; CBP 328) (C). CBP indicates carboplatin; MEL, melphalan.

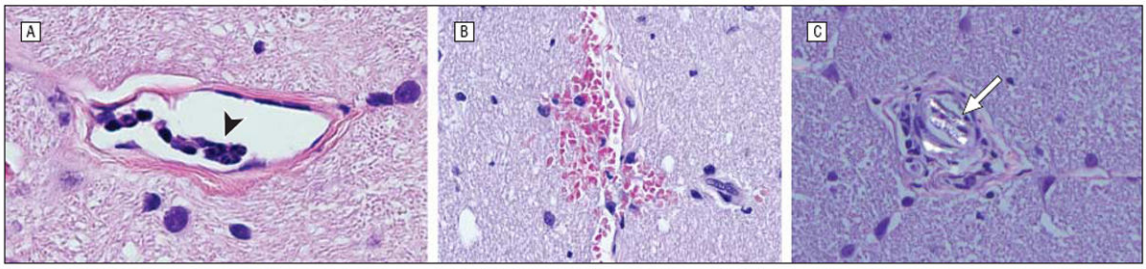

Figure 9.

Optic nerve findings include leukostasis (arrowhead) within the pial vessels (hematoxylin-eosin, original magnification ×80; MEL 330 (A), hemorrhage (hematoxylin-eosin, original magnification ×80; CBP 404) (B), and a polarizable foreign body (arrow) (hematoxylin-eosin, original magnification ×80; MEL 330) (C). CBP indicates carboplatin; MEL, melphalan.

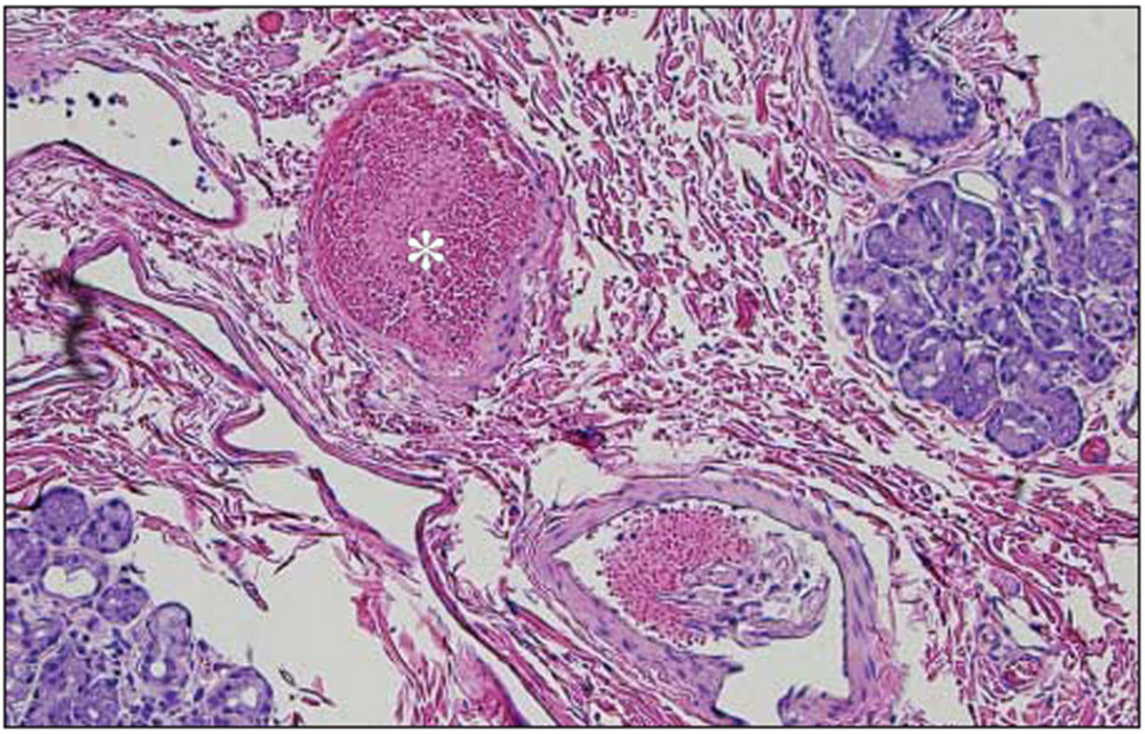

Figure 10.

Congestion and possible fibrin (asterisk) in vessels in the eyelid artery; note presence of accessory lacrimal glands and evidence of exfoliated endothelial cells in the lower right corner (hematoxylin-eosin, original magnification ×20; MEL 561). MEL indicates melphalan.

Table 1

Ocular Pathologic Findings in Nonhuman Primate Eyes After Superselective Intraopthalmic Artery Chemotherapy

Pathologic Finding	Location	No. of Eyes Affected	Treatment Cohort (Animal Identifier)	Representative Figure
Endothelial cell injury, leukocyte adhesion, and arteriole occlusion	Retinal arterioles	6 of 6	Melphalan and carboplatin (all animals)	1
Nerve fiber layer infarcts with edema of the ganglion cells and associated cytoid bodies	Retina	6 of 6	Melphalan and carboplatin (all animals)	3
Arteriole wall thickening, leukocyte adhesion, arteriole occlusion, and patchy, mixed inflammatory response	Choroidal and short posterior ciliary arteries	6 of 6	Melphalan and carboplatin (all animals)	4 and 5A
Disruption of internal elastic lamina with associated granulomatous inflammation	Choroidal arteriole	1 of 6	Carboplatin (CBP 039)	4C
Birefringent foreign bodies	Retinal, choroidal, and short posterior ciliary arteries	3 of 6	Melphalan (MEL 330) and carboplatin (CBP 328 and CBP 039)	5
Thrombi with denaturing and aggregation of erythrocytes	Laminar and postlaminar central retinal artery	4 of 6	Melphalan (MEL 006 and MEL 561) and carboplatin (CBP 328 and CBP 039)	6

Table 2

Orbital and Optic Nerve Pathologic Findings in Nonhuman Primate Eyes After Superselective Intraophthalmic Chemotherapy

Pathologic Finding	Location	No. of Eyes Affected	Treatment Cohort (Animal Identifier)	Representative Figure
Intimal hyperplasia	Ophthalmic artery	3	Melphalan (MEL 006 and MEL 561) and carboplatin (CBP 039)	8A
Fracturing of internal elastic lamina	Ophthalmic artery	2	Carboplatin (CBP 328 and CBP 039)	…
Leukostasis	Ophthalmic artery	2	Melphalan (MEL 330 and MEL 006)	…
Dissection within artery wall	Distal ophthalmic artery	1	Carboplatin (CBP 328)	8B and 8C
Reactive membrane lining lamina	Ophthalmic artery	1	Melphalan (MEL 561)	…
Thrombosis	Central retinal artery	1	Carboplatin (CBP 404)	…
Leukostasis and hemorrhage	Optic nerves	2	Melphalan (MEL 330) and carboplatin (CBP 328)	9A and 9B
Birefringent foreign bodies	Optic nerves	1	Melphalan (MEL 006) and carboplatin (CBP 404)	9C
Foreign body giant cell	Retrobulbar segment of optic nerve	1	Melphalan (MEL 330)	9